Communication
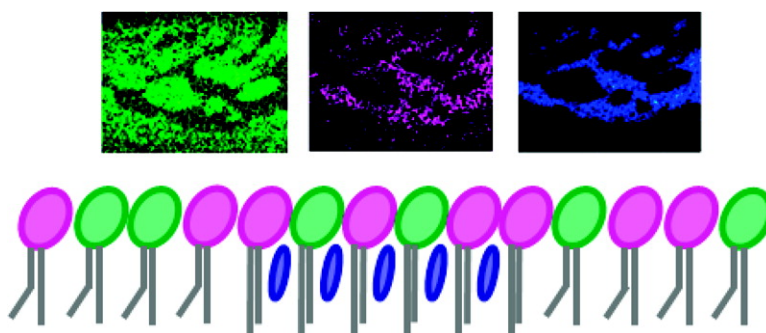
Sphingomyelin/Phosphatidylcholine and Cholesterol Interactions Studied by Imaging Mass Spectrometry

Leiliang Zheng, Carolyn M. McQuaw, Andrew G. Ewing, and Nicholas Winograd

More About This Article

Additional resources and features associated with this article are available within the HTML version:

- Supporting Information
- Links to the 6 articles that cite this article, as of the time of this article download
- Access to high resolution figures
- Links to articles and content related to this article
- Copyright permission to reproduce figures and/or text from this article

View the Full Text HTML

Sphingomyelin/Phosphatidylcholine and Cholesterol Interactions Studied by Imaging Mass Spectrometry
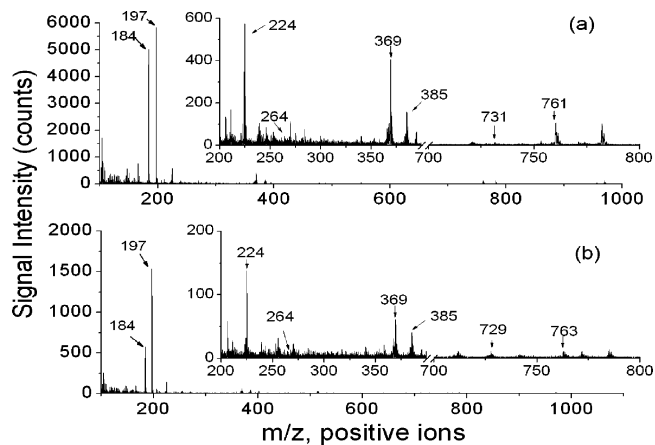
Leiliang Zheng, Carolyn M. McQuaw,[†] Andrew G. Ewing, and Nicholas Winograd*

Department of Chemistry, The Pennsylvania State University, University Park, Pennsylvania 16802

Received June 7, 2007; E-mail: nxw@psu.edu

Cell membranes are composed of a complex array of lipids, which play diverse roles in membrane dynamics, protein regulation, and signal transduction. It is important to understand how these lipids interact with each other and with other membrane components in order to better comprehend membrane functions. Many techniques are available to study lipid−lipid interactions such as solid-state NMR,[1,2] X-ray diffraction,[3,4] and various fluorescence-related techniques.[5,6] Recently, time-of-flight secondary ion mass spectrometry (TOF-SIMS) has been proven useful in identification of lipids in both model membrane systems and cellular membranes.[7−10] Here, we present label-free molecule-specific images which elucidate the nature of lipid−lipid interactions in three-component cellular membrane mimics. Our results show that sphingomyelin (SM) inclusion into cholesterol (CH) domains is driven by the phospholipid acyl chain saturation rather than by hydrogen bonding between SM and CH. Ternary mixtures composed of CH, SM, and phosphatidylcholine (PC) are investigated as mimics of the cellular membrane. TOF-SIMS images are acquired from supported Langmuir−Blodgett (LB) films with varying SM and PC acyl chain saturation; either, both, or neither contains one double bond at the same position. The images clearly show that acyl chain saturation is the dominating factor in determining phase separation.

The phospholipids used include *N*-stearoyl SM (SSM), 1-palmitoyl-2-oleoyl-*sn*-glycero-3-phosphocholine (POPC), *N*-oleoyl SM (OSM), and 1-palmitoyl-2-stearoyl-*sn*-glycero-3-phosphocholine (PSPC). The LB films used for investigation are 23% CH/47% SM/30% PC, and include the variants CH/SSM/POPC, CH/OSM/PSPC, CH/SSM/PSPC, and CH/OSM/POPC. The solutions of each combination were applied to the air−water interface, compressed to 7 mN/m, and then transferred onto hydrophilic substrates. This relatively low pressure is used to ensure the appearance of immiscible liquid phases and to ensure that the size of the domains is large enough for SIMS observation. Each combination was repeated in triplicate for reproducibility. The mass spectra of CH/SSM/POPC and CH/OSM/PSPC LB films are shown in Figure 1. Characteristic fragments include; [M − OH]+ at a mass-to-charge ratio (*m/z*) 369 for cholesterol, a sphingosine backbone fragment [C17H30ON]+ at *m/z* 264 for both SMs, and a peak at *m/z* 224 for both PCs which is a fragment [C8H19NPO4]+ of the PC headgroup plus part of the glycerol backbone (Figure S1). The molecular ions are [M − H]+ at *m/z* 385 for CH; [M + H]+ at *m/z* 761, 763 for POPC and PSPC, respectively; and M+ at *m/z* 729, 731 for OSM and SSM, respectively. [Note that none of substrate peaks overlap with these lipid peaks, Figure S3.] Since CH, SM, and PC are identified in each film by TOF-SIMS, molecule-specific images identify the location of each lipid, and representative images are presented in Figure 2 with their total ion images. CH/OSM/POPC and CH/SSM/PSPC are homogeneous with all lipid components evenly distributed (Supporting Information, Figure S2). However,

† Current Address: Vollum Institute and Department of Microbiology and Immunology, Oregon Health and Science University, Portland, Oregon 97220.


Figure 1. Secondary ion mass spectra of supported LB films: (a) 23% CH/47% SSM/30% POPC, (b) 23% CH/47% OSM/30% PSPC.

domain structures are observed for the films of CH/SSM/POPC and CH/OSM/PSPC (Figure 2). [Note that substrate images are in the Supporting Information, Figure S3, and the uniformity of the images confirms that there is no substrate-induced domain formation.] Lipid localization is also confirmed by line scans (Figure 2). The molecule-specific images for the CH/SSM/POPC films show that CH is colocalized with SSM in the domain and that POPC is excluded from these areas. For CH/OSM/PSPC, however, PSPC colocalizes with the CH domains, and OSM is excluded. The secondary ion intensities of CH and the colocalized lipid are close to zero outside the CH-rich domain area. However, lipid exclusion is not complete since a residual intensity is still observed in the CH-poor areas.

In the cellular membrane, CH is a major component, and SMs are predominantly saturated, whereas PCs are mainly unsaturated. It has been hypothesized that CH and SM form lateral heterogeneities in the plane of membranes (rafts) and that they are of functional significance (i.e., signaling or sorting platforms). While the concept is still under debate, many studies have aimed at understanding the interaction between CH and SM, especially relative to the interactions between CH and PC (a nonraft lipid species). One difference between SM and PC lipid classes lies in the head−tail linkage region. The long-chain fatty acids of PCs are linked to the glycerol backbone via ester groups, whereas SMs have a long-chain sphingoid base with an amide-linked chain. Thus, SMs are more polar in this region and can effectively hydrogen bond to CH via its amine and hydroxyl groups more than PCs can. This intermolecular hydrogen bonding has been speculated to contribute to preferential interactions between CH and SM.[2,11,12] However, other groups report no specificity between CH and SM, but rather that a higher level of acyl chain saturation in SM facilitates the hydrophobic match between SM and CH, thus driving them to colocalize in the biomembrane.[13,14]
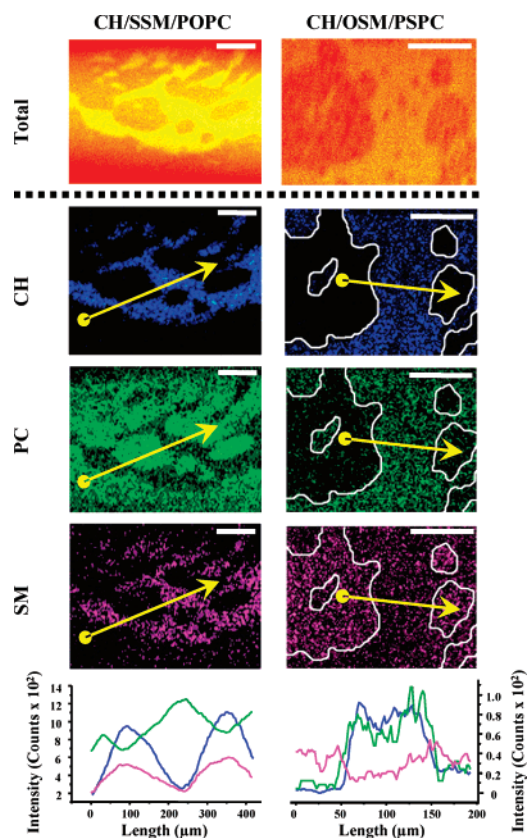
Figure 2. TOF-SIMS images of the two supported lipid three-component LB films. The scale bar represents 100 μm. The total ion images are 256 × 256 pixels and the molecular specific images are 128 × 128 pixels, with 40 shots/pixel. CH (blue), PC (green), and SM (pink) are represented by m/z 369, m/z 224, and m/z 264, respectively. Similar patterns are observed in replicate experiments as seen, for example, in Figure S4. The line scans shown below represent the intensity variation along the yellow arrows superimposed on the SIMS images, both with respect to the length and the direction. More details are given in the Supporting Information.

Model membranes containing CH, SM, and PC have been widely used in CH−SM interaction studies, and phase separation has been observed by fluorescence microscopy[6,15] and atomic force microscopy.[16] In our experiments, the SMs and PCs were specifically chosen to have the same number of carbons on both acyl chains so that they only differ by the linkage of the 16-carbon chain to the headgroup and by the saturation of the other 18-carbon chain. Without the need for labels, molecule-specific images reported here show that when SM and PC are both saturated or both unsaturated all the lipids are evenly distributed in the film, and CH domains do not form. Thus, CH does not differentiate between SM and PC by their head−tail linkage. However, when SM and PC differ by a double bond placed in the middle of the 18-carbon chain, CH domains are observed in the film due to phase separation, which means CH interacts with one lipid significantly more strongly than the other. Clearly, CH favors the lipid that has saturated acyl chains, and this preference is strong enough to localize the saturated lipids into CH domains and to exclude the unsaturated lipid. Cholesterol is known to have a condensing effect on other lipids, which can be explained by the hydrophobic match between the steroid ring of CH and the acyl chains of other lipids.[17] Lipids with saturated acyl chains can interact more closely with CH than those with unsaturated acyl chains since the double bond produces a kink in the middle of the carbon chain that sterically prevents half of the chain from interacting with CH. Our results show that one double bond in the acyl chain is enough to change the lipid interaction with CH, regardless of the difference in the head−tail linkage region of SM

and PC. The results also suggest that the SM−CH interaction is dominated by the hydrophobic match of acyl chains, and that hydrogen bonding between the amide or the sphingoid of SM and the −OH group of CH does not contribute significantly to the total interaction. McConnell has proposed a condensing complex model which suggests, in a ternary mixture, the formation of "condensed complexes" between cholesterol and saturated lipids, and the complex is immiscible with the unsaturated lipids.[18] Our results show that CH preferentially interacts with lipids through the saturated acyl chain which may indeed indicate the formation of complexes. However, as noted above, the exclusion of the unsaturated lipids from CH domains is not complete. Hence, if the condensing complexes form in our ternary systems, they are not 100% immiscible with the unsaturated lipids.

In conclusion, using TOF-SIMS we have observed the label-free lipid localization determined by acyl chain saturation and its effect on CH domain formation. The result indicates that the high saturation level of SM acyl chains in the cellular membrane is the important driving force for SM colocalization with CH in lipid rafts. Other possible specific interactions between sphingoid- or amide-linkage groups and CH are not observed. This study also extends the use of label-free mass spectrometry imaging to understanding complex biological interactions at the molecular level.

Supporting Information Available: Instrumental information, molecular structures of the lipids, and additional SIMS images and spectra. This material is available free of charge via the Internet at http://pubs.acs.org.

References

(1) Hao, Y. H.; Chen, J. W. *J. Membr. Biol.* **2001**, *183*, 85−92.
(2) van Duyl, B. Y.; Ganchev, D.; Chupin, V.; de Kruijff, B.; Killian, J. A. *FEBS Lett.* **2003**, *547*, 101−106.
(3) Holopainen, J. M.; Lemmich, J.; Richter, F.; Mouritsen, O. G.; Rapp, G.; Kinnunen, P. K. J. *Biophys. J.* **2000**, *78*, 2459−2469.
(4) Shaikh, S. R.; Cherezov, V.; Caffrey, M.; Soni, S. P.; LoCascio, D.; Stillwell, W.; Wassall, S. R. *J. Am. Chem. Soc.* **2006**, *128*, 5375−5383.
(5) Veatch, S. L.; Polozov, I. V.; Gawrisch, K.; Keller, S. L. *Biophys. J.* **2004**, *86*, 2910−2922.
(6) Stottrup, B. L.; Stevens, D. S.; Keller, S. L. *Biophys. J.* **2005**, *88*, 269−276.
(7) Bourdos, N.; Kollmer, F.; Benninghoven, A.; Ross, M.; Sieber, M.; Galla, H. J. *Biophys. J.* **2000**, *79*, 357−369.
(8) Sostarecz, A. G.; McQuaw, C. M.; Ewing, A. G.; Winograd, N. *J. Am. Chem. Soc.* **2004**, *126*, 13882−13883.
(9) McQuaw, C. M.; Sostarecz, A. G.; Zheng, L. L.; Ewing, A. G.; Winograd, N. *Langmuir* **2005**, *21*, 807−813.
(10) Ostrowski, S. G.; Van Bell, C. T.; Winograd, N.; Ewing, A. G. *Science* **2004**, *305*, 71−73.
(11) Smaby, J. M.; Brockman, H. L.; Brown, R. E. *Biochemistry* **1997**, *36*, 2338.
(12) Bittman, R.; Kasireddy, C. R.; Mattjus, P.; Slotte, J. P. *Biochemistry* **1994**, *33*, 11776−11781.
(13) Epand, R. M.; Epand, R. F. *Chem. Phys. Lipids* **2004**, *132*, 37−46.
(14) Holopainen, J. M.; Metso, A. J.; Mattila, J. P.; Jutila, A.; Kinnunen, P. K. J. *Biophys. J.* **2004**, *86*, 1510−1520.
(15) Veatch, S. L.; Keller, S. L. *Biophys. J.* **2003**, *85* (5), 3074−3083.
(16) Rinia, H. A.; de Kruijff, B. *FEBS Lett.* **2001**, *504*, 194−199.
(17) Ohvo-Rekila, H.; Ramstedt, B.; Leppimaki, P.; Slotte, J. P. *Prog. Lipid Res.* **2002**, *41*, 66−97.
(18) McConnell, H. M. *Biophys. J.* **2005**, *88* (4), L23−L25.

JA0741675